AMERICAN SOCIETY FOR MICROBIOLOGY | Applied and Environmental Microbiology®

PLANT MICROBIOLOGY

Succinate Transport Is Not Essential for Symbiotic Nitrogen Fixation by *Sinorhizobium meliloti* or *Rhizobium leguminosarum*

Michael J. Mitsch,[a] George C. diCenzo,[a] Alison Cowie,[a] Turlough M. Finan[a]

[a]Department of Biology, McMaster University, Hamilton, Ontario, Canada

ABSTRACT Symbiotic nitrogen fixation (SNF) is an energetically expensive process performed by bacteria during endosymbiotic relationships with plants. The bacteria require the plant to provide a carbon source for the generation of reductant to power SNF. While C_4-dicarboxylates (succinate, fumarate, and malate) appear to be the primary, if not sole, carbon source provided to the bacteria, the contribution of each C_4-dicarboxylate is not known. We address this issue using genetic and systems-level analyses. Expression of a malate-specific transporter (MaeP) in *Sinorhizobium meliloti* Rm1021 *dct* mutants unable to transport C_4-dicarboxylates resulted in malate import rates of up to 30% that of the wild type. This was sufficient to support SNF with *Medicago sativa*, with acetylene reduction rates of up to 50% those of plants inoculated with wild-type *S. meliloti*. *Rhizobium leguminosarum* bv. viciae 3841 *dct* mutants unable to transport C_4-dicarboxylates but expressing the *maeP* transporter had strong symbiotic properties, with *Pisum sativum* plants inoculated with these strains appearing similar to plants inoculated with wild-type *R. leguminosarum*. This was despite malate transport rates by the mutant bacteroids being 10% those of the wild type. An RNA-sequencing analysis of the combined *P. sativum-R. leguminosarum* nodule transcriptome was performed to identify systems-level adaptations in response to the inability of the bacteria to import succinate or fumarate. Few transcriptional changes, with no obvious pattern, were detected. Overall, these data illustrated that succinate and fumarate are not essential for SNF and that, at least in specific symbioses, L-malate is likely the primary C_4-dicarboxylate provided to the bacterium.

IMPORTANCE Symbiotic nitrogen fixation (SNF) is an economically and ecologically important biological process that allows plants to grow in nitrogen-poor soils without the need to apply nitrogen-based fertilizers. Much research has been dedicated to this topic to understand this process and to eventually manipulate it for agricultural gains. The work presented in this article provides new insights into the metabolic integration of the plant and bacterial partners. It is shown that malate is the only carbon source that needs to be available to the bacterium to support SNF and that, at least in some symbioses, malate, and not other C_4-dicarboxylates, is likely the primary carbon provided to the bacterium. This work extends our knowledge of the minimal metabolic capabilities the bacterium requires to successfully perform SNF and may be useful in further studies aiming to optimize this process through synthetic biology approaches. The work describes an engineering approach to investigate a metabolic process that occurs between a eukaryotic host and its prokaryotic endosymbiont.

KEYWORDS *Sinorhizobium*, cross-kingdom interactions, dicarboxylate, endosymbionts, malic acid, metabolic engineering, metabolism, nitrogen fixation, nutrient transport, transcriptome

Received 18 July 2017 **Accepted** 31 August 2017

Accepted manuscript posted online 15 September 2017

Citation Mitsch MJ, diCenzo GC, Cowie A, Finan TM. 2018. Succinate transport is not essential for symbiotic nitrogen fixation by *Sinorhizobium meliloti* or *Rhizobium leguminosarum*. Appl Environ Microbiol 84:e01561-17. https://doi.org/10.1128/AEM.01561-17.

Editor Rebecca E. Parales, University of California, Davis

Address correspondence to Turlough M. Finan, finan@mcmaster.ca.

The rhizobia are a group of bacteria capable of fixing atmospheric nitrogen gas to ammonia in symbiosis with legume plants. Following entry into the plant cells of the legume nodule, the rhizobia are surrounded by a plant-derived membrane, called the peribacteroid membrane, and differentiate into nitrogen-fixing bacteroids. Nitrogen fixation is a highly energetic process that requires 8 e^-, 8 H^+, and 16 mol of ATP per mole of N_2 reduced to 2(NH_4) (1). The evidence is consistent with plant-derived C_4-dicarboxylates (malate, succinate, and fumarate) fulfilling this role (see reference 2 for a review of nodule metabolism). The photosynthate sucrose is diverted to the nodule, where plant sucrose synthases cleave the sucrose into glucose and fructose that then enters glycolysis (Fig. 1) (3). Carbon from glycolysis and carbon dioxide is then funneled into C_4-dicarboxylates primarily through the activities of phosphoenolpyruvate (PEP) carboxylases, which convert PEP and carbonic acid into oxaloacetate (OAA), and malate dehydrogenases, which convert OAA into L-malate that can be further converted into L-fumarate and L-succinate (Fig. 1) (4, 5). Notably, malate dehydrogenase activity is elevated in nodules compared to in other plant tissues due to the presence of nodule-enhanced malate dehydrogenases that are expressed specifically in the nodule and located in the cytoplasm and have higher affinities for OAA and NADH than other malate dehydrogenases. This appears to favor catalysis of the reaction in the direction of OAA to malate (5–7). The C_4-dicarboxylates must then cross both the peribacteroid membrane and the bacteroid membrane, where their metabolism is believed to provide the ATP and reductant requirements needed for nitrogen fixation by the oxygen-sensitive nitrogenase enzyme (Fig. 1) (8–10).

The C_4-dicarboxylate transport system of rhizobia consists of three proteins, namely, DctA, DctB, and DctD (reviewed in reference 11). DctA is the transport protein, while DctB and DctD constitute a two-component regulatory system, where DctB is the histidine kinase and DctD is the response regulator. Although DctA is primarily thought of as a transporter of C_4-dicarboxylate, it can also transport additional substrates, including aspartate and orotate (12, 13). DctA functions as a symporter, likely transporting two protons per C_4-dicarboxylate, meaning the pH difference between the alkaline bacteroid and acidic peribacteroid space can drive C_4-dicarboxylate import during symbiosis (14, 15). Mutations of *dctA*, *dctB*, or *dctD* result in an ineffective symbiosis incapable of any nitrogen fixation (9, 10).

Although the evidence for plant-derived C_4-dicarboxylates as the main carbon source available to N_2-fixing bacteroids is compelling, it is unclear what the relative contributions of each C_4-dicarboxylate are, i.e., malate, fumarate, and succinate. Depending on the plant species, the concentration of malate in the nodule was determined to be ~6- to 9.3-fold higher than that of succinate, and ~3.2- to 8.7-fold higher than that of fumarate (16–18). As the measured metabolite concentrations are an average from all of the plant tissue, the actual metabolite concentrations in the infected plant's cells and the concentrations surrounding bacteroids are uncertain. In a recent study, the concentration of malate in purified *Rhizobium leguminosarum* bacteroids was ~55-fold higher than that in free-living *R. leguminosarum* cells, in comparison to those of succinate and fumarate, which are 2.5- and 26-fold higher in bacteroids relative to those in free-living cells, respectively (19). Depending on the study, the K_m and V_{max} of succinate and malate transport across the peribacteroid membrane are similar and the transporter is likely saturated during symbiosis (8, 20). Likewise, there is little difference in the transport kinetics of malate and succinate by rhizobial DctA proteins, although the maximal rate of succinate import may be 2-fold higher than that of malate (8, 10, 15, 17, 21). These observations are consistent with malate accumulation in both the plant and bacterial partners during the symbiosis and indirectly support malate as the predominate C_4-dicarboxylate provided to bacteroids during symbiosis. However, the relative contribution of each C_4-dicarboxylate during symbiosis has not been experimentally evaluated.

The MaeP protein of *Streptococcus gallolyticus* (formerly *Streptococcus bovis*) is similar to the DctA protein of rhizobia, in that it is a membrane symporter that cotransports its substrate with protons (22). However, MaeP is a malate-specific trans-

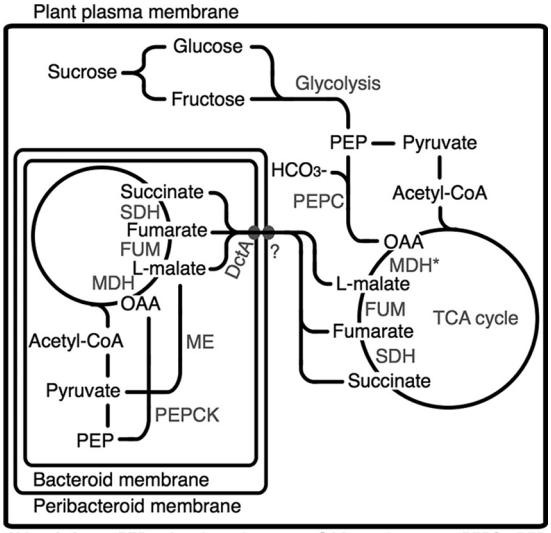

FIG 1 Nodule carbon metabolism. A schematic representation of the primary nodule carbon metabolic pathways is shown. Sucrose in the plant cytosol is split into glucose and fructose, which are then catabolized via glycolysis to phosphoenolpyruvate (PEP). Carbon from PEP and carbonic acid is diverted to oxaloacetate (OAA) and L-malate via PEP-carboxylase and the nodule-enhanced malate dehydrogenase, and then possibly to fumarate, and succinate. These metabolites then cross both the peribacteroid and bacteroid membranes, which requires DctA, where their metabolism provides the ATP and reductant required to power the nitrogenase reaction. TCA, tricarboxylic acid.

porter that is unable to recognize succinate or fumarate as substrates (22). Here, we expressed the *maeP* gene in *dct* mutants of *Sinorhizobium meliloti* 1021 and *R. leguminosarum* bv. viciae 3841 and examined the symbiotic capabilities of these strains. We show that, although the rate of malate transport by MaeP is only a fraction of the malate transport rate of DctA, MaeP was sufficient to support low rates of nitrogen fixation by *S. meliloti* with *Medicago sativa* and nearly wild-type levels of nitrogen fixation by *R. leguminosarum* with *Pisum sativum*. Moreover, integrated plant-bacterium nodule RNA-sequencing was consistent with the *R. leguminosarum-P. sativum* symbiosis being naturally adapted to malate serving as the primary C_4-dicarboxylate available to *R. leguminosarum*.

RESULTS

Expression of *maeP* in *S. meliloti* supports moderate rates of malate transport. *S. meliloti* does not contain a *maeP* gene ortholog, and four constructs were prepared to express the *S. gallolyticus maeP* gene in *S. meliloti* (see Materials and Methods). The *maeP* gene was placed under the control of either the *S. meliloti dme* promoter (P_{dme}-*maeP*) or the *S. meliloti dctA* promoter (P_{dctA}-*maeP*) and was either integrated into the *S. meliloti* genome in a single copy (ΦP_{dme}-*maeP* and ΦP_{dctA}-*maeP*) or expressed from a medium-copy-number plasmid (P_{dme}-*maeP* and P_{dctA}-*maeP*). Each construct was transferred to two independent *dctA* mutants (23) to examine the ability of the four constructs to facilitate malate transport in *S. meliloti*.

All strains grew at rates similar to that of the *dctA*$^+$ wild-type strain when provided with glucose as the sole source of carbon (Table 1). In contrast to the *dctA*$^+$ wild-type strain, none of the *dctA* mutant strains, with or without *maeP*, were capable of growth when provided with succinate or fumarate as the sole source of carbon (Table 1). In contrast, all four *maeP* constructs supported various rates of growth with L-malate as the sole carbon source (Table 1). These results were consistent with MaeP transporting L-malate but not succinate or fumarate. The single-copy ΦP_{dme}-*maeP* construct supported growth with a doubling time approximately twice that of the *dctA*$^+$ strain, while

TABLE 1 Phenotypic effects of *maeP* expression in *S. meliloti*

Genotype	Generation time (h) when grown with[a]:				Malate uptake (nmol/min/mg protein)[b]		Symbiotic assay[c]			
							Expt I		Expt II	
	Glucose	Succinate	Fumarate	Malate	No competitor	With succinate	SDW (mg)	ARA (nmol/min)	SDW (mg)	ARA (nmol/min)
dctA$^+$	3.4 ± 0.1	3.2 ± 0.0	2.9 ± 0.3	3.0 ± 0.0	24.7 ± 1.4	2.4 ± 0.5	131.8 ± 9.5	1,089 ± 254	79.2 ± 1.8	458 ± 67
dctA14	3.6 ± 0.3	0.0 ± 0.0	0.0 ± 0.0	0.0 ± 0.0	0.1 ± 0.1	0.1 ± 0.0	10.1 ± 0.6	0 ± 0	8.7 ± 0.3	1.3 ± 0.1
dctA26	3.8 ± 0.1	0.0 ± 0.0	0.0 ± 0.0	0.0 ± 0.0	ND[d]	ND	10.3 ± 1.0	0 ± 0	9.7 ± 1.2	2.1 ± 0.6
dctA14 ΦP_{dme}-*maeP*[e]	3.7 ± 0.1	0.0 ± 0.0	0.0 ± 0.0	7.3 ± 0.0	2.1 ± 0.1	1.6 ± 0.3	11.1 ± 0.6	8 ± 6	ND	ND
dctA26 ΦP_{dme}-*maeP*	3.3 ± 0.1	0.0 ± 0.0	0.0 ± 0.0	6.5 ± 0.0	ND	ND	12.2 ± 1.1	4.3 ± 0.4	ND	ND
dctA14 P_{dme}-*maeP*	4.2 ± 0.0	0.0 ± 0.0	0.0 ± 0.0	3.3 ± 0.0	4.8 ± 0.1	4.8 ± 0.0	33.9 ± 4.3	416 ± 3	ND	ND
dctA26 P_{dme}-*maeP*	3.9 ± 0.0	0.0 ± 0.0	0.0 ± 0.0	3.1 ± 0.0	ND	ND	30.5 ± 5.5	498 ± 18	ND	ND
dctA14 ΦP_{dctA}-*maeP*	3.8 ± 0.0	0.0 ± 0.0	0.0 ± 0.0	4.2 ± 0.0	5.2 ± 0.1	5.5 ± 0.1	ND	ND	10.9 ± 0.1	7 ± 1
dctA26 ΦP_{dctA}-*maeP*	4.0 ± 0.0	0.0 ± 0.0	0.0 ± 0.0	4.4 ± 0.0	ND	ND	ND	ND	9.8 ± 2.0	5 ± 1
dctA14 P_{dctA}-*maeP*	4.4 ± 0.1	0.0 ± 0.0	0.0 ± 0.0	3.4 ± 0.0	7.7 ± 0.2	7.3 ± 0.2	ND	ND	23.6 ± 1.6	227 ± 79
dctA26 P_{dctA}-*maeP*	4.3 ± 0.0	0.0 ± 0.0	0.0 ± 0.0	3.2 ± 0.0	ND	ND	ND	ND	21.3 ± 1.3	143 ± 4
Uninoculated							11.0 ± 1.0	ND	9.3 ± 1.8	ND

[a]Generation time when grown with the indicated carbon substrate. Values are means from duplicate samples ± ranges.
[b]Rate of malate uptake in the presence of either just 40 μM radiolabeled malate (no competitor) or 40 μM radiolabeled malate plus 800 μM unlabeled succinate. Values are means from triplicate samples ± standard errors.
[c]Results from two symbiotic assays are presented. In experiment I, alfalfa plants were harvested 38 days postinoculation (dpi) with *S. meliloti*; for experiment II, plants were harvested 43 days postinoculation (dpi) with *S. meliloti*. SDW, shoot dry weight; ARA, acetylene reduction activity. Values are means from triplicate samples ± standard errors.
[d]ND, not determined.
[e]Φ, construct was integrated into the genome through single-crossover plasmid integrant. The absence of this symbol indicates that the construct is expressed from a multicopy replicative pBBR1 vector.

increasing the copy number facilitated growth at nearly wild-type levels (Table 1). Similarly, the doubling time of *dctA* mutants carrying the ΦP_{dctA}-*maeP* construct was approximately 50% longer than that of the wild type, but growth was similar to the wild type when the copy number was increased (Table 1).

L-Malate uptake assays revealed that *dctA* mutant strains carrying ΦP_{dme}-*maeP* transported L-malate at a rate ~8.5% that of the wild-type *dctA*$^+$ strain, and increasing the P_{dme}-*maeP* copy number by expression from the replicative vector resulted in an increase in the L-malate transport rate to ~19.4% that of the wild type (Table 1). Higher rates of L-malate transport were observed when *maeP* was expressed from the *dctA* promoter; the ΦP_{dctA}-*maeP* construct facilitated L-malate transport at a rate ~21.1% that of the wild type, while expression from a replicative vector increased the transport rate to ~31.2% that of the wild type (Table 1). Moreover, whereas succinate inhibited L-malate transport by DctA, the inclusion of succinate in the transport assays had little effect on L-malate transport by MaeP expressed from any of the four constructs (Table 1). Together, the growth and transport assays indicated that MaeP was capable of transporting L-malate, but not succinate or fumarate, when expressed in free-living *S. meliloti*.

MaeP supports low rates of N_2 fixation by *S. meliloti* during symbiosis with alfalfa. To examine whether malate uptake, in the absence of succinate and fumarate transport, was sufficient to support symbiotic nitrogen fixation by *S. meliloti*, *M. sativa* (alfalfa) plants were inoculated with the various *dctA* mutants expressing the *maeP* malate permease gene. Little nitrogen fixation was observed when *maeP* was present as a single-copy genome integrant regardless of the promoter. The acetylene reduction activities of plants inoculated with these strains were less than 2% of those inoculated with wild-type *S. meliloti* (Table 1), and the shoot dry weights were indistinguishable from those inoculated with the *dctA* mutants (Table 1). In contrast, moderate rates of nitrogen fixation were observed when *maeP* was expressed from the multicopy vector. Regardless of the promoter, shoot dry weights of plants inoculated with these strains were ~23 to 30% those of plants inoculated with the wild type (Table 1; Fig. 2), while acetylene reduction activities of the root systems were between ~31 and 50% those of plants inoculated with the wild type (Table 1). These data indicated that succinate and fumarate transport is nonessential for symbiotic nitrogen fixation with alfalfa and that

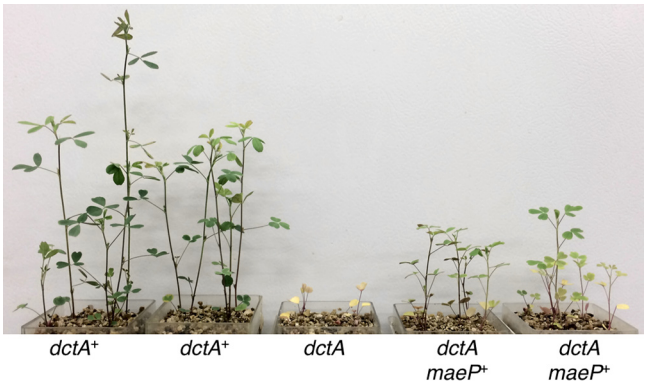

FIG 2 Alfalfa plants inoculated with *S. meliloti*. Alfalfa plants were imaged 53 days postinoculation with *S. meliloti*. Strains: *dctA*$^+$, wild-type *S. meliloti*; *dctA*, *dctA14*::Tn*5*; *dctA maeP*$^+$, *dctA14*::Tn*5*, multicopy P_{dctA}::*maeP*.

malate transport at the rates mediated by MaeP was sufficient for at least moderate rates of nitrogen fixation.

Malate transport supports high rates of N_2 fixation in the *R. leguminosarum*-pea symbiosis. To examine the ability of MaeP to support nitrogen fixation in other symbioses, *maeP* was next introduced into two *dct* mutants of *R. leguminosarum* bv. viciae 3841. Both the P_{dme}-*maeP* and P_{dctA}-*maeP* constructs in the multicopy vector were introduced into *R. leguminosarum dctA*::ΩSp and Δ*dctABD*::ΩSp mutants (24). In most cases, *maeP* facilitated growth of the mutants with L-malate as a sole source of carbon, but not with succinate or fumarate (Table 2). In fact, the *dct* mutants expressing *maeP* appeared to grow more rapidly with L-malate than did the wild type (Table 2). The sole exception was the P_{dctA}-*maeP* constructs in the *dctABD* mutant, which failed to grow with L-malate, presumably as no expression from the *dctA* promoter occurred in the absence of the DctB and DctD regulatory proteins (23, 25).

P. sativum (pea) cv. Lincoln plants were inoculated with the *R. leguminosarum* strains to examine the ability of MaeP to support nitrogen fixation during this symbiosis. The

TABLE 2 Phenotypic effects of *maeP* expression in *R. leguminosarum* bv. viciae

Genotype	Generation time (h) when grown with[a]:				Bacteroid malate uptake (nmol/min/mg protein)[b]		Symbiotic assay[c]	
	Glucose	Succinate	Fumarate	Malate	No competitor	With succinate	SDW (mg)	ARA (nmol/min)
Expt I								
dctA$^+$	9.4 ± 0.5	8.8 ± 0.0	10.0 ± 0.1	9.7 ± 0.1	6.56 ± 0.39	0.39 ± 0.00	576 ± 41	1,641 ± 465
dctA	9.7 ± 0.1	0.0 ± 0.0	0.0 ± 0.0	0.0 ± 0.0	0.27 ± 0.03	0.00 ± 0.00	297 ± 9	6 ± 5
Δ*dctABD*	9.8 ± 0.1	0.0 ± 0.0	0.0 ± 0.0	0.0 ± 0.0	0.27 ± 0.00	0.00 ± 0.00	320 ± 13	0 ± 0
dctA P_{dme}-*maeP*	11.6 ± 0.1	0.0 ± 0.0	0.0 ± 0.0	5.7 ± 0.1	0.56 ± 0.04	0.60 ± 0.08	485 ± 43	726 ± 128
Δ*dctABD* P_{dme}-*maeP*	11.2 ± 0.1	0.0 ± 0.0	0.0 ± 0.0	5.5 ± 0.1	0.56 ± 0.01	0.52 ± 0.02	483 ± 32	752 ± 101
dctA P_{dctA}-*maeP*	12.0 ± 0.4	0.0 ± 0.0	0.0 ± 0.0	5.5 ± 0.1	ND[d]	ND	ND	ND
Δ*dctABD* P_{dctA}-*maeP*	11.1 ± 0.3	0.0 ± 0.0	0.0 ± 0.0	0.0 ± 0.0	ND	ND	ND	ND
Uninoculated							185 ± 35	ND
Expt II								
dctA$^+$	ND	ND	ND	ND	7.61 ± 1.60	0.67 ± 0.28	409 ± 71	1,081 ± 70
dctA	ND	ND	ND	ND	0.16 ± 0.06	0.12 ± 0.0	259 ± 8	0 ± 0
Δ*dctA* P_{dctA}-*maeP*	ND	ND	ND	ND	0.75 ± 0.06	0.56 ± 0.02	422 ± 98	1,169 ± 273
Uninoculated							280 ± 12	ND

[a]Generation time when grown with the indicated carbon substrate. Values are means from duplicate samples ± ranges.
[b]Bacteroid malate uptake in the presence of 40 μM radiolabeled malate (no competitor) or 40 μM radiolabeled malate plus 800 μM unlabeled succinate. Bacteroids were isolated from pea root nodules of plants 40 days postinoculation (dpi) with *R. leguminosarum*. Values are means from triplicate samples ± standard errors.
[c]Results from two symbiotic assays are presented. In experiment I, pea plants were harvested 41 days postinoculation (dpi) with *R. leguminosarum*; for experiment II, plants were harvested 42 days postinoculation (dpi) with *R. leguminosarum*. SDW, pea shoot dry weight; ARA, acetylene reduction activity. Values are means from triplicate samples ± standard errors.
[d]ND, not determined.

P_{dme}-*maeP* construct supported nitrogen fixation at a rate ~45% that of a *dctA*$^+$ strain on the basis of both shoot dry weights and acetylene reduction activities (Table 2). Strikingly, the expression of *maeP* from the *dctA* promoter in a *dctA* mutant resulted in a symbiotic performance that was indistinguishable from that of a *dctA*$^+$ strain in terms of both shoot dry weights and acetylene reduction activities (Table 2). Malate uptake assays were performed with bacteroids purified from pea nodules to examine the rate of malate transport by the various strains. Malate uptake by bacteroids containing the P_{dme}-*maeP* construct imported malate at a rate ~8.5% that of bacteroids containing the wild-type *dctA* gene (Table 2). Surprisingly, the malate uptake rate by bacteroids with the P_{dctA}-*maeP* construct was only slightly higher, at ~10% that of the wild type (Table 2). However, we cannot rule out that the apparent low rate of transport by the *maeP*-expressing strains was a consequence of these mutant bacteroids being more leaky/compromised or due to increased respiration and conversion of ^{14}C into CO_2 by the mutants. Nevertheless, these data overall supported that malate transport alone was sufficient for a highly effective *R. leguminosarum*-pea symbiosis and that succinate and fumarate transport was dispensable.

For the RNA-sequencing experiment described below, *P. sativum* cv. Homesteader plants were used. As before, plants inoculated with the *R. leguminosarum dctA* mutants carrying the P_{dctA}-*maeP* construct appeared dark green and very healthy, although they were slightly, but noticeably, smaller than plants inoculated with the wild type (Fig. 3A). Similarly, the effective pink nodules induced by the *dctA* mutant carrying P_{dctA}-*maeP* were on average only slightly smaller than those induced by wild-type cells. The smaller shoot and nodule sizes were presumably due, in part, to the loss of the P_{dctA}-*maeP* plasmid in a portion of the cells, as ~10 to 15% of nodules were ineffective and formed by cells that had lost the plasmid (data not shown). Confocal microscopy of nodule sections revealed that nodules containing the *dctA* mutant with the P_{dctA}-*maeP* construct were structurally similar to those containing wild-type *R. leguminosarum*, and in both cases, the nodules were filled with rhizobial cells (Fig. 3H versus J, and K versus M). This was in contrast to nodules induced by the *dctA* mutant that displayed signs of senescence (Fig. 3I and L). However, nodule sections from nodules filled with *R. leguminosarum* expressing the *maeP* malate permease displayed much greater iodine staining in the nitrogen-fixing zone than sections from nodules filled with the wild type (Fig. 3D versus B, and G versus E), which was indicative of elevated levels of starch accumulation. Hence, while MaeP-mediated malate transport appeared largely sufficient for normal nodule development, the increased starch accumulation suggested the bacteroids of these nodules may have been unable to use all the carbon normally available to *R. leguminosarum* bacteroids.

Transcriptomic analysis of pea nodules. Given that *P. sativum* plants inoculated with the *R. leguminosarum dctA* mutant containing the P_{dctA}-*maeP* construct appeared quite healthy, a transcriptomic analysis was performed to examine whether there were any system-level adaptations to accommodate the inability of the bacteroids to import succinate. Total RNA was isolated from *P. sativum* nodules formed by either wild-type *R. leguminosarum* or the *R. leguminosarum dctA* mutant containing the P_{dctA}-*maeP* construct, and RNA-sequencing was performed on biological triplicates. On average, ~4.5-fold more sequencing reads mapped to the *P. sativum* transcriptome than to the *R. leguminosarum* genes. The ratios were statistically significantly similar between treatments, 4.2 $\pm$ 0.3 (standard deviation) for the wild type versus 4.9 $\pm$ 0.1 for P_{dctA}-*maeP* (*P* value of 0.077 using a two-tailed Student's *t* test), indicating that the ratio of plant to bacterial cells in nodules was not significantly influenced by the inability of the bacteroids to transport succinate.

Euclidian distance analysis followed by hierarchical clustering analysis indicated that each set of triplicates clustered together, as expected, regardless of whether all features were considered at once (Fig. 4) or if the plant and bacterial features were examined independently (see Fig. S1 in the supplemental material). The high interreplicate distances relative to the intertreatment distances suggested that, although divergent,

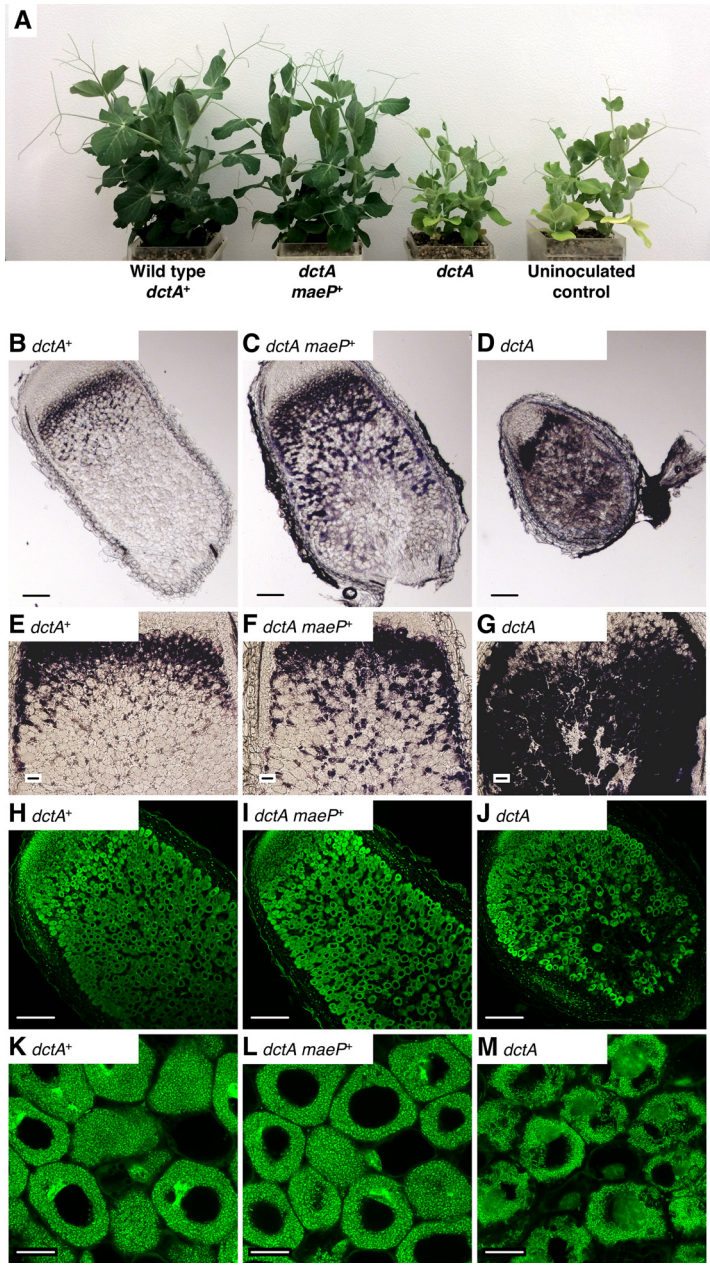

FIG 3 Symbiotic phenotypes of pea plants inoculated with *R. leguminosarum*. Pea plants were harvested 25 days postinoculation with *R. leguminosarum*. (A) Images of the shoots of the pea plants. (B to G) Images of nodule sections visualized with bright-field microscopy following iodine staining. (H to M) Confocal microscopy images of nodule sections stained with the nucleic acid binding dye Syto9. Strains: *dctA*$^+$, wild-type *R. leguminosarum* bv. viciae; *dctA maeP*$^+$, *dctA*::ΩSp^r, multicopy P_{dctA}::*maeP*; *dctA*, *dctA*::ΩSp^r.

the differences in the transcriptional patterns of the two sets of nodules were relatively small (Fig. 4). Only 42 *R. leguminosarum* genes were differentially expressed more than 2-fold, while only a six-gene operon (*RL0979-RL0984*), encoding an uncharacterized ABC transport system showing similarity to polyamine transporters, was differentially expressed more than 4-fold (see Data Set S1). Additionally, only 20 plant transcripts were differentially expressed more than 2-fold, while only the *P. sativum* Ps*Cam020853* transcript, encoding a putative sulfate transporter, was differentially expressed more than 4-fold (see Data Set S2).

Not much of a pattern was observed in the functional role of the differentially regulated gene sets; indeed, 18 (43%) of the differentially expressed *R. leguminosarum*

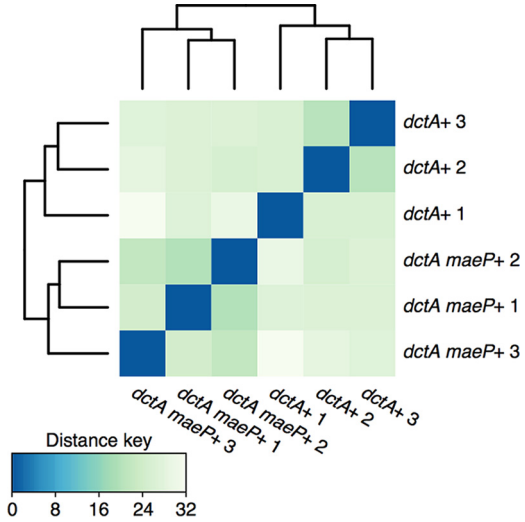

FIG 4 RNA-sequencing sample distance analysis. RNA-sequencing count tables were statistically analyzed with DESeq2 (57), and the Euclidean distances were calculated between each sample. Samples were clustered using hierarchical clustering analysis, and the dendrograms represent the clustering results. The heatmap illustrates the pairwise distances between the indicated samples, with the colors indicating the distances as shown in the key in the bottom left; i.e., the more blue the square, the more similar the samples.

genes were annotated with the term hypothetical, while 11 (55%) of the differentially expressed *P. sativum* genes were not annotated by Mercator (Data Sets S1 and S2). Little difference was observed in the expression of plant or bacterial central carbon metabolic genes (Table 3), and similarly, most bacterial *nif* and *fix* genes were changed very little (Table 3). This analysis revealed that the lack of succinate/fumarate transport by bacteroids resulted in few transcriptional perturbations, consistent with the nodule system being naturally well adapted to malate serving as the primary bacteroid carbon source.

DISCUSSION

We undertook genetic and systems-level approaches to examine the contribution of malate to symbiotic nitrogen fixation relative to the other C_4-dicarboxylates, succinate and fumarate. By replacing the DctA C_4-dicarboxylate transporter of two rhizobia with the MaeP protein specific for malate, it was possible to specifically examine the ability of malate to support symbiotic nitrogen fixation. The inability of the MaeP-expressing strains to transport succinate or use succinate as a sole carbon source, as well as the inability of these strains to grow with fumarate as a sole carbon source, confirmed that MaeP was specific to malate transport in both *S. meliloti* and *R. leguminosarum*.

MaeP was observed to support nitrogen fixation by *S. meliloti* during symbiosis with *M. sativa*, albeit much less efficiently than the wild-type *dctA*$^+$ *S. meliloti* (Table 1; Fig. 2). It was therefore concluded that succinate and fumarate transport was dispensable during this symbiosis so long as malate transport remained. As MaeP also did not appear to transport L-aspartate (data not shown), these data further confirm that the symbiotic requirement of DctA is independent of its L-aspartate transport function (12). However, it remains unclear why only low rates of nitrogen fixation were shown by the *S. meliloti dctA* mutant expressing *maeP*. The rate of malate transport by MaeP in *S. meliloti* free-living cells was less than a third of the malate transport rate by DctA (Table 1); thus, simply increasing the rate of malate transport to the maximal rate achieved by DctA may be sufficient to restore full symbiotic nitrogen fixation. Alternatively, fumarate transport and/or succinate transport may be required for maximal efficiency of this symbiosis. The concentration of malate in *M. sativa* nodules is approximately four times the combined concentrations of fumarate plus succinate (17). The inability to transport these latter compounds may therefore

TABLE 3 Transcription of select bacterial and plant genes in pea nodules with bacteria expressing *maeP* versus *dctA*

Gene or transcript	Function	*dctA maeP*$^+$ vs *dctA*$^+$[a]	
		Expression (%)	Adjusted *P* value
R. leguminosarum bv. viciae 3841			
sdhB	Succinate dehydrogenase subunit	79	1.72E−03
fumC	Fumarase	80	6.22E−02
mdh	Malate dehydrogenase	80	7.27E−03
icd	Isocitrate dehydrogenase	85	2.43E−01
pckA	PEP carboxykinase	97	9.46E−01
dme	NAD^+ malic enzyme	87	2.97E−01
pgk	Phosphoglycerate kinase	87	5.94E−01
zwf1	Glucose-6-P dehydrogenase	92	8.01E−01
fixA	Electron transfer protein	57	1.57E−17
fixO1	Cytochrome oxidase subunit	77	3.05E−03
fixK	Transcriptional regulator	121	8.60E−02
fixN3	Cytochrome cbb_3 oxidase subunit	155	4.54E−03
nifA	Transcriptional activator	66	5.58E−09
nifK	Nitrogenase subunit	92	7.31E−01
amtB	Ammonium transporter	58	6.94E−05
glnK	Nitrogen regulatory protein PII	61	5.54E−03
glnII	Glutamine synthetase II	63	1.03E−03
P. sativum cv. Homesteader[b]			
Ps*Cam006660*	Succinate dehydrogenase subunit	96	9.23E−01
Ps*Cam060158*	Fumarase	93	8.50E−01
Ps*Cam045782*	Malate dehydrogenase	94	8.33E−01
Ps*Cam042881*	Isocitrate dehydrogenase	96	9.32E−01
Ps*Cam049188*	PEP carboxylase	90	5.93E−01
Ps*Cam044324*	Phosphoglycerate kinase	89	4.00E−01
Ps*Cam049115*	Glucose-6-P dehydrogenase	107	8.23E−01
Ps*Cam050530*	Phosphofructokinase	106	8.29E−01

[a]Expression values represent the expression level of the genes/transcripts in *P. sativum* nodules containing the *dctA maeP*$^+$ strain as percentages of the expression of the genes/transcripts in *P. sativum* nodules containing the *dctA*$^+$ strain. The adjusted *P* values for the comparisons are provided as well.
[b]For all *P. sativum* transcripts, the transcript with each annotated function that had the most mapped reads is provided as a representative.

represent a loss of ~20% of the available carbon substrates, a loss that is further amplified considering that the catabolism of succinate generates more reductant than does the catabolism of L-malate. This in turn would decrease the amount of reductant available to power the nitrogenase enzyme. Reduced transport would also result in reduced flux through the electron transport chain, potentially resulting in elevated oxygen concentrations that may decrease the activity of oxygen-sensitive nitrogenase (26). Further study is required to differentiate between these possibilities.

The situation was somewhat different in the *R. leguminosarum-P. sativum* symbiosis, where MaeP appeared nearly sufficient to functionally replace DctA. Plant shoot dry weights and acetylene reduction activities of *P. sativum* inoculated with a *dctA maeP*$^+$ strain were indistinguishable from those of *P. sativum* inoculated with the *dctA*$^+$ strain (Table 2; Fig. 3). This was true despite iodine staining that was suggestive of starch accumulation and the *dctA maeP*$^+$ bacteroids being incapable of utilizing all available carbon (Fig. 3), which may have been a consequence of the low rate of malate transport into bacteroids by MaeP relative to that by DctA (Table 2). A transcriptomics approach was employed to examine whether any systems-level adaptations at the level of the transcriptome were required to support nitrogen fixation solely by malate. We predicted that if the bacteroids received large quantities of succinate or fumarate from the host, the inability of bacteroids to transport these compounds would have resulted in metabolic disturbances that would be reflected in the nodule transcriptome. This was not seen. Few differences were observed in the bacterial or plant transcriptome of nodules containing *R. leguminosarum* expressing *maeP* in place of *dctA*, and no major pattern of the changes was detected. However, in the P_{dctA}-*maeP* strain, there was a slight increase in expression of *fixN3*, encoding a cytochrome cbb_3 oxidase, whereas there was a minor decrease in the expression of the *fixABCX-nifAB* gene cluster, which

encodes the NifA transcriptional regulator and the FixABCX electron transport-related proteins, although these genes remained among the most highly expressed in the bacteroid (Table 3). Whether these changes are biologically meaningful is unclear, but they could reflect a change in the redox state due to decreased flux through succinate dehydrogenase, which produces a $FADH_2$ molecule, and slightly elevated O_2 concentrations due to less flux through the electron transport chain (26). Alternatively, the increased expression of the FixN3 cytochrome oxidase subunit may also suggest enhanced respiration by the *maeP*-expressing bacteroids, and further research is needed to evaluate this possibility. If true, this may partially explain the apparent low L-malate uptake rates, as the increased respiration would result in greater loss of ^{14}C to CO_2, and thus lower scintillation counts. There was also somewhat lower expression of *amtB* (ammonium transport), *glnK* (nitrogen regulatory protein PII), and *glnII* (glutamine synthetase II), which are all regulated by the NtrBC system (27, 28), in the P_{dctA}-*maeP* strain, potentially suggestive of a disturbance in nitrogen balance (Table 3).

Previous comparative metabolic profiling indicated that relative to free-living cells, *R. leguminosarum* bacteroids in *P. sativum* nodules accumulate malate to a greater extent than they do succinate or fumarate (19). Although not examined in *P. sativum* nodules, the concentration of malate present in all nodule systems tested is much higher than the concentrations of succinate and fumarate (16–18, 29), including in the *R. leguminosarum* symbiotic partner *Phaseolus vulgaris* (29). Additionally, a *Rhizobium tropici dct* mutant with an alternate transporter able to import succinate, but not malate or fumarate, fixed only low rates of nitrogen in symbiosis with *P. vulgaris* (30, 31); however, it was possible that this phenotype was due to the transporter being poorly expressed or active in the bacteroid. When these previous indirect lines of evidence are considered together with the plant phenotypes and transcriptomics data presented here, the evidence is consistent with malate naturally serving as the primary C_4-dicarboxylate provided to the bacteroids, while succinate and fumarate play secondary roles, at least in the *R. leguminosarum-P. sativum* symbiosis.

It was somewhat surprising that the symbiotic phenotypes of the *S. meliloti* and *R. leguminosarum dctA* mutants expressing the *maeP* gene were so different from each other (Fig. 2 and 3). One possibility is that expression of *maeP* in *S. meliloti* had pleiotropic effects, such as membrane destabilization, that may have impaired the symbiosis; future work is required to eliminate this possibility. Additionally, high expression of the non-codon-optimized *maeP* gene may have resulted in pleiotropic effects and the relatively low efficiency of malate uptake by MaeP compared to that by DctaA; however, as the codon usages of *S. meliloti* and *R. leguminosarum* are similar, such effects are expected to be similar in both organisms. A second possibility is that the difference reflects differences in the functioning of the symbioses. It is not uncommon for mutations of orthologous genes to yield divergent phenotypes, depending on which symbiosis is examined (32–36), such as with mutations in the phosphoenolpyruvate carboxykinase and malic enzyme genes, whose products are involved in C_4-dicarboxylate metabolism (for example, see references 32 and 37). The different outcomes of the symbioses studied here may therefore reflect differences in the ratios of carbon sources provided to the bacteroids and in the overall metabolic integration of the two symbiotic partners.

It is interesting that rhizobial *dct* mutants are completely unable to fix any nitrogen, as observed here (Tables 1 and 2; Fig. 2 and 3) and elsewhere (9, 10). Surely, the rhizobia must receive at least small amounts of other compounds that can be catalyzed as a carbon and energy source, such as L-proline and γ-aminobutyrate (GABA) (38, 39); yet, C_4-dicarboxylates are absolutely essential for symbiotic nitrogen fixation. We hypothesize that there is a minimum threshold of energy production that is required to sustain nitrogen fixation and that below this threshold, nitrogen fixation fails to occur. *S. meliloti dctA* mutants carrying the single copy ΦP_{dme}-*maeP* and ΦP_{dctA}-*maeP* constructs essentially failed to fix nitrogen despite mediating low rates of malate transport (Table 1). Similarly, *S. meliloti* strains containing DctA proteins with reduced, but not zero, ability to transport C_4-dicarboxylates failed to fix nitrogen in symbiosis with *M. sativa* (40). Moreover, the

slightly higher malate transport rate by *R. leguminosarum* bacteroids with the P_{dctA}-*maeP* construct compared to the P_{dme}-*maeP* construct was translated into significantly greater nitrogen fixation (Table 2). Perhaps nitrogen fixation only occurs once the basal metabolic needs of the bacteroid are fulfilled. Alternatively, it may be that a minimum flux of electrons through the electron transport chain is required to produce the low-oxygen environment required for nitrogenase activity. At least in free-living diazotrophs, a decrease in the rate of cellular respiration results in elevated oxygen concentrations and a decrease in nitrogenase activity (26). This could explain why there is not a linear relationship between C_4-dicarboxylate transport and nitrogen fixation.

This work provides direct experimental evidence consistent with malate serving as the predominate C_4-dicarboxylate received from the host during the *R. leguminosarum-P. sativum* symbiosis, and it also reinforces the interpretation that the symbiotic phenotype of *dctA* mutants is a consequence of the inability to transport C_4-dicarboxylates instead of some other unidentified consequence of the *dctA* mutations. In future work, it will be interesting to replace the DctA transporters of several rhizobia with a variety of transporters specific to malate and other C_4-dicarboxylates to further dissect the relative contribution of each of the substrates and to examine the variability of phenotypes between symbioses.

MATERIALS AND METHODS

Bacterial strains, growth conditions, and genetic techniques. The compositions of LB, LB supplemented with $MgSO_4$ and $CaCl_2$ (LBmc), tryptone-yeast extract (TY), and MM9 minimal medium (41), as well as M9 minimal medium (42) and MOPS (morpholinepropanesulfonic acid) minimal medium (15) were as described before. LB was used for the growth of *Escherichia coli*, and was incubated at 37°C. *S. meliloti* was grown using LBmc, MM9, or M9 medium at 30°C, while *R. leguminosarum* was grown using TY or MOPS medium at 30°C. Carbon sources in minimal medium were included at a final concentration of 10 mM and included D-glucose, succinate, fumarate, and L-malate. Antibiotic concentrations for *S. meliloti* were 200 μg/ml streptomycin, 200 μg/ml neomycin, and 20 μg/ml gentamicin, and the same concentrations of streptomycin and gentamicin were used for *R. leguminosarum*. Standard molecular biology techniques and triparental conjugations were performed as described previously (42, 43). All strains and plasmids are listed in Table 4.

Cloning of *maeP*. The malate permease *maeP* gene of *S. gallolyticus* was PCR amplified from the pSK4 vector (22) using the primers 5′-GAA ATA GCA TGC AAA AGA AAT TGC CC-3′ and 5′-AGC GGA TAA CAA TTT CAC ACA GGA-3′. The PCR product was digested with SphI/KpnI and ligated into SphI/KpnI digested plasmid pTH400, a pUC119 derivative that contained the *S. meliloti dme* promoter sequence (44), resulting in plasmid pTH449 that contained the *maeP* gene expressed from the *S. meliloti dme* promoter. The P_{dme}-*maeP* fragment was isolated from pTH449 via digestion with HindIII and KpnI, and was ligated into HindIII/KpnI-digested pUCP30T (45) to produce pTH461, as well as into HindIII/KpnI-digested pBBR1MCS-5 (46) to produce pTH600.

To express the *maeP* gene under the control of the *S. meliloti dctA* promoter, the *dctA-dctB* intergenic region was PCR amplified from the plasmid pTH31 (23) using the primers 5′-ATG AGC ATG CTA TCC TCC AC-3′ and 5′-GGA AGC TTG ACC ATG CG-3′. The resulting 250-bp PCR product was digested with HindIII and SphI and ligated into HindIII/SphI-digested pTH461 (see above), replacing the *dme* promoter with the *dctA* promoter, to yield plasmid pTH647. Plasmid pTH647 was digested with HindIII and KpnI to release the P_{dctA}-*maeP* fragment, which was then ligated into HindIII/KpnI-digested pBBR1MCS-5 to produce pTH648.

Derivatives of pUCP30T function as suicide vectors in *S. meliloti*, and the transfer of pTH449 (ΦP_{dme}-*maeP*) and pTH647 (ΦP_{dctA}-*maeP*) into *S. meliloti* resulted in the single copy integration of these genes into the genome via single-crossover recombination at the *dme* and *dctA* promoter regions, respectively. Derivatives of pBBR1MCS-5 are replicative medium-copy-number vectors in *S. meliloti* and *R. leguminosarum*, meaning the transfer of pTH600 (P_{dme}-*maeP*) and pTH648 (P_{dctA}-*maeP*) into these species resulted in the multicopy expression of these constructs.

Growth curves. Bacterial growth experiments were performed and analyzed essentially as described previously (41). Overnight cultures grown in LBmc or TY medium were pelleted and washed once with carbon-free M9 (*S. meliloti*) or MOPS (*R. leguminosarum*) medium, and then resuspended in carbon-free M9 or MOPS medium to an optical density at 600 nm (OD_{600}) of 1 in a 1-cm pathlength. Ten microliters of each cell suspension and 190 μl of M9 or MOPS medium with the desired carbon source were mixed in a well of a 96-well microtiter plate, and the plate was incubated at 30°C with shaking in a BioTek Cytation3 plate reader. The doubling times of *S. meliloti* cultures were calculated between OD_{600} values of 0.1 and 0.3 (not corrected for pathlength), while the doubling times of *R. leguminosarum* cultures were calculated between OD_{600} values of 0.05 and 0.12 (not corrected for pathlength).

Transport assays. Transport assays were performed according to a described method (15). For assays involving free-living *S. meliloti*, 50 ml of overnight M9-glucose cultures was pelleted and washed three times with TAS solution (40 mM MOPS, 20 mM KOH, 4 mM $MgSO_4$, 20 mM NH_4CL, 0.2 mM $CaCO_3$,

TABLE 4 Bacterial strains and plasmids

Strain or plasmid	Characteristics[a]	Reference or source
Sinorhizobium meliloti strains		
Rm1021	Wild-type SU47 *str-21*; Sm^r	60
RmF642	Rm1021 *dctA14*::Tn*5*; Sm^r Nm^r	23
RmF647	Rm1021 *dctA26*::Tn*5*; Sm^r Nm^r	23
RmK298	Rm1021(pBBR1mcs-5); Sm^r Gm^r	This study
RmK301	RmF642(pBBR1mcs-5); *dctA14*::Tn*5* pBBR1mcs-5	This study
RmK302	RmF647(pBBR1mcs-5); *dctA26*::Tn*5* pBBR1mcs-5	This study
RmH948	RmF642(pTH461); *dctA14*::Tn*5* ΦP_{dme}-*maeP*	This study
RmH949	RmF647(pTH461); *dctA26*::Tn*5* ΦP_{dme}-*maeP*	This study
RmK299	RmF642(pTH600); *dctA14*::Tn*5* P_{dme}-*maeP*	This study
RmK300	RmF647(pTH600); *dctA26*::Tn*5* P_{dme}-*maeP*	This study
RmK380	RmF642(pTH647); *dctA14*::Tn*5* ΦP_{dctA}-*maeP*	This study
RmK381	RmF647(pTH647); *dctA26*::Tn*5* ΦP_{dctA}-*maeP*	This study
RmK376	RmF642(pTH648); *dctA14*::Tn*5* P_{dctA}-*maeP*	This study
RmK377	RmF647(pTH648); *dctA26*::Tn*5* P_{dctA}-*maeP*	This study
Rhizobium leguminosarum bv. viciae strains		
3841	Wild type; Sm^r	61
RU714	3841 Δ*dctABD*::ΩSp^r	24
RU727	3841 *dctA*::ΩSp^r	24
RlK367	3841(pBBR1mcs-5); Δ*dctABD*::ΩSp pBBR1mcs-5	This study
RlK368	RU714(pBBR1mcs-5); Δ*dctABD*::ΩSp pBBR1mcs-5	This study
RlK369	RU727(pBBR1mcs-5); *dctA*::ΩSp pBBR1mcs-5	This study
RlK370	RU714(pTH600); Δ*dctABD*::ΩSp P_{dme}-*maeP*	This study
RlK371	RU727(pTH600); *dctA*::ΩSp P_{dme}-*maeP*	This study
RlK378	RU714(pTH648); Δ*dctABD*::ΩSp P_{dctA}-*maeP*	This study
RlK379	RU727(pTH648); *dctA*::ΩSp P_{dctA}-*maeP*	This study
Plasmids		
pBBR1mcs-5	Replicative vector in the rhizobia; Gm^r	46
pUCP30T	Suicide vector in the rhizobia; Gm^r	45
pSK4	Template for *maeP*; Amp^r	22
pTH31	Source of the *dctA* promoter; Tc^r	23
pTH400	pUC119 derivative with the *dme* promoter; Amp^r	44
pTH449	pTH400 with *maeP* following the *dme* promoter; Amp^r	This study
pTH461	pUCP30T with P_{dme}-*maeP*; Gm^r	This study
pTH600	pBBR1mcs-5 with P_{dme}-*maeP*; Gm^r	This study
pTH647	pUCP30T with P_{dctA}-*maeP*; Gm^r	This study
pTH648	pBBR1mcs-5 with P_{dctA}-*maeP*; Gm^r	This study

[a]Sm, streptomycin; Sp, spectinomycin; Nm, neomycin; Gm, gentamicin; Tc, tetracycline; Amp, ampicillin. The *maeP* gene was placed under the control of either the *S. meliloti dme* promoter (P_{dme}-*maeP*) or the *S. meliloti dctA* promoter (P_{dctA}-*maeP*) and was either integrated into the *S. meliloti* genome in single-copy (ΦpUCP30T with P_{dme}-*maeP* and ΦpUCP30T with P_{dctA}-*maeP*) or expressed from a medium-copy-number pBBR1 plasmid (P_{dme}-*maeP* and P_{dctA}-*maeP*).

0.1 mM NaCl, 1.2 mM K_2HPO_4, 0.4 mM KH_2PO_4, pH 7.0), and then resuspended in TAS solution to 20 mg of cell pellet per ml of TAS solution.

For assays involving *R. leguminosarum* bacteroids, nodules of *P. sativum* plants were collected and ground to a slurry in cold MMS buffer (40 mM MOPS, 20 mM KOH, 2 mM $MgSO_2$, 0.3 M sucrose, pH 7.0) using a mortar and pestle and kept on ice for the remainder of the procedure. The slurry was filtered through four layers of cheese cloth and collected in a 15-ml centrifuge tube. The suspension was centrifuged at 250 × *g* at 4°C for 10 min, and the supernatant was transferred to a fresh tube and centrifuged a second time as before. The supernatant was collected and centrifuged at 3,900 × *g* at 4°C for 10 min to pellet the bacteroids. The bacteroids were washed three times with 5 ml MMS buffer, resuspended and centrifuged, and then resuspended to 30 mg/ml in MMS buffer and kept on ice for at most 3 h prior to performing the transport assays.

Transport assays were performed using radiolabeled L-[U-^{14}C]malic acid (Amersham). A 100-μl aliquot of bacteroid or cell suspension was mixed with 280 μl MMS buffer and incubated in a 30°C water bath for 5 min. Assays were initiated by the addition of 20 μl of 0.8 mM L-malate for a final concentration of 40 μM with a specific activity of 55 Ci · mol^{-1}. Samples were removed at the desired time points and placed on presoaked 0.45-μm-pore-size nitrocellulose membranes (Millipore) in a vacuum manifold, which were immediately rinsed with 5 to 10 ml of MMS buffer and dried under a heat lamp. All assays were performed in triplicate, and three time points were analyzed per sample from 1 to 6 min.

In experiments involving inhibitor compounds, 100 μl of cell or bacteroid suspension was added to 260 μl MMS buffer and incubated at 30°C for 5 min. Twenty microliters of 16 mM succinate (final concentration of 800 μM) was added to each reaction, and the assays were initiated 15 s later by the addition of 20 μl of 0.8 mM L-malate (final concentration of 40 μM). Assays were continued as described above.

Symbiotic assays. Alfalfa (*M. sativa* cv. Iroquois) seeds were sterilized, germinated, and planted in Leonard assemblies (47) as described previously (23). Each *S. meliloti* strain was inoculated in triplicate pots containing 10 to 12 seedlings each, and plants were grown in a Conviron growth chamber as described before (23) for the indicated number of days. Acetylene reduction activity was measured using three root systems per pot as described elsewhere (23), and the plant shoots were collected and dried at 50°C to determine shoot dry weights. Twenty-five randomly chosen nodules were crushed in LBmc plus 300 mM sucrose, and bacteria were isolated by plating on LBmc with streptomycin. Phenotypes of the nodule isolates were examined by replica plating 30 colonies on M9 medium with succinate, malate, or glucose as the sole carbon source, and on LBmc medium plus gentamicin.

For most experiments involving pea plants, *P. sativum* cv. Leonard seeds were used. Seeds were surface sterilized by treatment with 2.5% hypochlorite for 30 min followed by treatment with 95% ethanol for 30 min. Seeds were rinsed with sterile distilled water for 2 h and then soaked in water overnight to hydrate the seeds. Seeds were germinated on 1% water agar plates and germinated for 72 h at room temperature in the dark. Five seedlings were planted per Leonard assembly and inoculated 48 h later with *R. leguminosarum* as described for *S. meliloti* (23). Acetylene reduction activity and shoot dry weights were determined as described above for alfalfa. Twenty-five randomly chosen nodules were crushed in TY plus 300 mM sucrose medium, bacteria were isolated by plating on TY medium with streptomycin, and plasmid retention was examined by replica plating 10 colonies on TY medium with gentamicin.

For microscopy work and RNA isolation, *P. sativum* cv. Homesteader seeds were used. Seeds were prepared and planted in Leonard assemblies with 250 ml Jensen's medium (48) as described elsewhere (49). Three seedlings were planted per Leonard assembly. Plants were routinely watered with sterile distilled water and once with 200 ml sterile Jensen's medium 21 days postinoculation with *R. leguminosarum*. Nodules were collected 25 days postinoculation with *R. leguminosarum*.

Microscopy. Nodules were collected, fixed with glutaraldehyde, and sectioned as described previously (33). Nodule sections were stained with Syto9 and visualized with confocal microscopy as described elsewhere (33). Iodine staining was performed largely as described before (50). Nodule sections were cleared with 6% hypochlorite for 20 s, washed with distilled water, stained with 0.1 M potassium iodine for 20 s, and again washed with distilled water. Sections were visualized under bright-field microscopy using a Nikon TE2000 inverted microscope.

RNA isolation. Nodules were collected from pea plants 25 days postinoculation with *R. leguminosarum*. Plants were removed from the vermiculite-sand mixture, and nodules were picked from the roots and immediately flash frozen in liquid nitrogen. Each biological replicate consisted of nodules from the three plants of a single Leonard assembly, and enough nodules were collected to fill a 2-ml centrifuge tube to approximately the 500-μl mark. Three biological replicates were prepared per strain, and nodules were stored at −80°C until use.

For RNA isolation, all nodules per sample were placed in an autoclaved mortar together with 800 μl of 1% β-mercaptoethanol in nuclease-free water (Bioshop) and immediately crushed using an autoclaved pestle. Approximately 500 μl of crushed nodule solution was transferred to a 1.5-ml centrifuge tube on ice and mixed with 500 μl of room temperature hot phenol solution (per 6 ml: 5 ml of hot phenol buffer [20 mM Tris-HCl pH 7.5, 400 mM NaCl, 40 mM EDTA, 1% SDS, in nuclease-free double-distilled water {ddH_2O}] and 1 ml unbuffered phenol). The mixtures were vigorously vortexed for 20 s and then immediately incubated in a water bath at 95°C for 1 min. RNA purification from these mixtures was then performed as described elsewhere (62) with two rounds of DNase I treatment. The quality of the RNA preparations was determined by gel electrophoresis using MOPS-formaldehyde-agarose gels, and the absence of genomic DNA was confirmed by PCR using primers that amplified the *R. leguminosarum bacA* gene (5′-CGA AAC GAG AGT GCC GTC CCG TGT TTC ATT CCT TCT TCC-3′ and 5′-CCG CCT TCT GAT GCC CGC CGT CAA CCG TCG GCG TGC AC-3′).

RNA sequencing and analysis. Depletion of rRNA, cDNA synthesis, and cDNA sequencing were performed at the Farncombe Family Digestive Health Research Institute, located at McMaster University. Depletion of rRNA was performed using Ribo-Zero rRNA removal kits (Illumina) with a 50:50 mix of bacterial and plant rRNA probes, and efficient rRNA depletion was confirmed using a BioAnalyzer run (Agilent Genomics). Sequencing was performed using one lane of an Illumina HiSeq with V3 technology and 50-nucleotide (nt) single-end reads. The absence of adapter sequences in the raw reads, the high quality at all nucleotide positions of the reads, and the absence of low-quality reads were confirmed with FastQC (51).

The annotated *P. sativum* cv. Camphor transcriptome (52) was downloaded, and the high- and low-copy-number files were concatenated into a single FASTA file. The nucleotide FASTA file of the coding regions of the GenBank assembly of the *R. leguminosarum* bv. viciae 3841 genome (53) was also downloaded. All nucleotide sequences from both organisms were combined into a single contiguous nucleotide FASTA file, the locations of all features were identified through a BLASTN search (54), and a corresponding gff file was prepared. In total, 53,171 features were considered: 45,908 *P. sativum* transcripts and 7,263 *R. leguminosarum* coding regions.

Raw sequencing reads were mapped to the combined FASTA file, described above, using Bowtie 2 with default settings (55), a read count summary table was prepared with HTSeq-count using the "-a 0" option (56), and differential expression was determined using DESeq2 (57). On average, 14.6 million reads mapped to *P. sativum* transcripts, 3.3 million reads mapped to *R. leguminosarum* coding regions, and 6.6 million reads failed to map. The high percentage of reads that were not mapped was presumably due in part to divergences between the transcriptome of *P. sativum* cv. Homesteader plants used in this study and the *P. sativum* cv. Camphor reference transcriptome.

The Euclidean distances between samples was determined with the *dist*(*t*(*assay*(*rld*))) function in R and were calculated from the log-transformed data obtained with the *rlog* function in R. Hierarchical clustering was performed with the *hclust* function in R. For calculation of the Euclidean distance between samples considering only the plant transcripts or only the bacterial genes, the count tables from HTseq-count were first split into two tables representing the plant and bacterial features, DESeq2 analysis was then performed separately on each set of data, and Euclidean distances were calculated as for the combined sample.

For functional annotation of the *P. sativum* transcripts, the peptide sequences that corresponded to the high- and low-copy-number transcripts were downloaded (52) and annotated using Mercator (58) and eggNOG-mapper (59). The functional annotation of the *R. leguminosarum* coding regions was obtained from the GenBank genome annotation (53).

Accession number(s). The complete set of analyzed data is provided in Data Sets S1, S2, S3 and S4 in the supplemental material, and the raw sequencing reads are available online at the Gene Expression Omnibus (accession: GSE101430).

SUPPLEMENTAL MATERIAL

Supplemental material for this article may be found at https://doi.org/10.1128/AEM.01561-17.

SUPPLEMENTAL FILE 1, PDF file, 0.2 MB.

SUPPLEMENTAL FILE 2, XLSX file, 5.9 MB.

ACKNOWLEDGMENTS

This work was supported by the National Science and Engineering Research Council of Canada through grants to T.M.F. and an NSERC CGS-D award to G.C.D. We are grateful to Shigeyuki Kawai for the *maeP* plasmid, pSK4.

REFERENCES

1. Hoffman BM, Lukoyanov D, Yang Z-Y, Dean DR, Seefeldt LC. 2014. Mechanism of nitrogen fixation by nitrogenase: the next stage. Chem Rev 114:4041–4062. https://doi.org/10.1021/cr400641x.
2. Udvardi M, Poole PS. 2013. Transport and metabolism in legume-rhizobia symbioses. Annu Rev Plant Biol 64:781–805. https://doi.org/10.1146/annurev-arplant-050312-120235.
3. Gordon A, Minchin F, James C, Komina O. 1999. Sucrose synthase in legume nodules is essential for nitrogen fixation. Plant Physiol 120:867–878. https://doi.org/10.1104/pp.120.3.867.
4. Schulze J, Shi L, Blumenthal J, Samac DA, Gantt JS, Vance CP. 1998. Inhibition of alfalfa root nodule phosphoenolpyruvate carboxylase through an antisense strategy impacts nitrogen fixation and plant growth. Phytochemistry 49:341–346. https://doi.org/10.1016/S0031-9422(98)00221-0.
5. Miller SS, Driscoll B, Gregerson RG, Gantt JS, Vance CP. 1998. Alfalfa malate dehydrogenase (MDH): molecular cloning and characterization of five different forms reveals a unique nodule-enhanced MDH. Plant J 15:173–184. https://doi.org/10.1046/j.1365-313X.1998.00192.x.
6. Schulze J, Tesfaye M, Litjens RHMG, Bucciarelli B, Trepp G, Miller S, Samac D, Allan D, Vance CP. 2002. Malate plays a central role in plant nutrition, p 133–139. *In* Horst WJ, Bürkert A, Claassen N, Flessa H, Frommer WB, Goldbach H, Merbach W, Olfs H-W, Römheld V, Sattelmacher B, Schmidhalter U, Schenk MK, von Wiŕen N (ed), Progress in plant nutrition: plenary lectures of the XIV International Plant Nutrition Colloquium. Springer, Dordrecht, Netherlands.
7. Appels MA, Haaker H. 1988. Identification of cytoplasmic nodule-associated forms of malate dehydrogenase involved in the symbiosis between *Rhizobium leguminosarum* and *Pisum sativum*. Euro J Biochem 171:515–522.
8. Udvardi MK, Price GD, Gresshoff PM, Day DA. 1988. A dicarboxylate transporter on the peribacteroid membrane of soybean nodules. FEBS Lett 231:36–40. https://doi.org/10.1016/0014-5793(88)80697-5.
9. Ronson CW, Lyttleton P, Robertson JG. 1981. C(4)-dicarboxylate transport mutants of *Rhizobium trifolii* form ineffective nodules on *Trifolium repens*. Proc Natl Acad Sci U S A 78:4284–4288. https://doi.org/10.1073/pnas.78.7.4284.
10. Finan TM, Wood JM, Jordan DC. 1983. Symbiotic properties of C4-dicarboxylic acid transport mutants of *Rhizobium leguminosarum*. J Bacteriol 154:1403–1413.
11. Yurgel SN, Kahn ML. 2004. Dicarboxylate transport by rhizobia. FEMS Microbiol Rev 28:489–501. https://doi.org/10.1016/j.femsre.2004.04.002.
12. Watson RJ, Rastogi VK, Chan YK. 1993. Aspartate transport in *Rhizobium meliloti*. J Gen Microbiol 139:1315–1323. https://doi.org/10.1099/00221287-139-6-1315.
13. Yurgel S, Mortimer MW, Rogers KN, Kahn ML. 2000. New substrates for the dicarboxylate transport system of *Sinorhizobium meliloti*. J Bacteriol 182:4216–4221. https://doi.org/10.1128/JB.182.15.4216-4221.2000.
14. Gutowski SJ, Rosenberg H. 1975. Succinate uptake and related proton movements in *Escherichia coli* K-12. Biochem J 152:647–654. https://doi.org/10.1042/bj1520647.
15. Finan TM, Wood JM, Jordan DC. 1981. Succinate transport in *Rhizobium leguminosarum*. J Bacteriol 148:193–202.
16. Streeter JG. 1987. Carbohydrate, organic acid, and amino acid composition of bacteroids and cytosol from soybean nodules. Plant Physiol 85:768–773. https://doi.org/10.1104/pp.85.3.768.
17. McRae DG, Miller RW, Berndt WB, Joy K. 1989. Transport of C4-dicarboxylates and amino acids by *Rhizobium meliloti* bacteroids. Mol Plant Microbe Interact 2:273–278. https://doi.org/10.1094/MPMI-2-273.
18. Stumpf DK, Burris RH. 1979. A micromethod for the purification and quantification of organic acids of the tricarboxylic acid cycle in plant tissues. Anal Biochem 95:311–315. https://doi.org/10.1016/0003-2697(79)90221-5.
19. Terpolilli JJ, Masakapalli SK, Karunakaran R, Webb IUC, Green R, Watmough NJ, Kruger NJ, Ratcliffe RG, Poole PS. 2016. Lipogenesis and redox balance in nitrogen-fixing pea bacteroids. J Bacteriol 198:2864–2875. https://doi.org/10.1128/JB.00451-16.
20. Ou Yang LJ, Udvardi MK, Day DA. 1990. Specificity and regulation of the dicarboxylate carrier on the peribacteroid membrane of soybean nodules. Planta 182:437–444. https://doi.org/10.1007/BF02411397.
21. San Francisco MJD, Jacobson GR. 1985. Uptake of succinate and malate in cultured cells and bacteroids of two slow-growing species of *Rhizobium*. J Gen Microbiol 131:765–773. https://doi.org/10.1099/00221287-131-4-765.
22. Kawai S, Suzuki H, Yamamoto K, Kumagai H. 1997. Characterization of the L-malate permease gene (*maeP*) of *Streptococcus bovis* ATCC 15352. J Bacteriol 179:4056–4060. https://doi.org/10.1128/jb.179.12.4056-4060.1997.
23. Yarosh OK, Charles TC, Finan TM. 1989. Analysis of C4-dicarboxylate transport genes in *Rhizobium meliloti*. Mol Microbiol 3:813–823. https://doi.org/10.1111/j.1365-2958.1989.tb00230.x.
24. Reid CJ, Walshaw DL, Poole PS. 1996. Aspartate transport by the Dct system in *Rhizobium leguminosarum* negatively affects nitrogen-regulated operons. Microbiology 142:2603–2612. https://doi.org/10.1099/00221287-142-9-2603.

25. Ronson CW, Astwood PM, Downie JA. 1984. Molecular cloning and genetic organization of C4-dicarboxylate transport genes from *Rhizobium leguminosarum*. J Bacteriol 160:903–909.
26. Goldberg I, Nadler V, Hochman A. 1987. Mechanism of nitrogenase switch-off by oxygen. J Bacteriol 169:874–879. https://doi.org/10.1128/jb.169.2.874-879.1987.
27. Taté R, Riccio A, Merrick M, Patriarca EJ. 1998. The *Rhizobium etli amtB* gene coding for an $NH4^+$ transporter is down-regulated early during bacteroid differentiation. Mol Plant Microbe Interact 11:188–198. https://doi.org/10.1094/MPMI.1998.11.3.188.
28. Patriarca EJ, Chiurazzi M, Manco G, Riccio A, Lamberti A, De Paolis A, Rossi M, Defez R, Iaccarino M. 1992. Activation of the *Rhizobium leguminosarum glnII* gene by NtrC is dependent on upstream DNA sequences. Mol Gen Genet 234:337–345. https://doi.org/10.1007/BF00538692.
29. Antoniw LD, Sprent JI. 1978. Primary metabolites of *Phaseolus vulgaris* nodules. Phytochemistry 17:675–678. https://doi.org/10.1016/S0031-9422(00)94207-9.
30. Batista S, Catalán AI, Hernández-Lucas I, Martínez-Romero E, Aguilar OM, Martínez-Drets G. 2001. Identification of a system that allows a *Rhizobium tropici dctA* mutant to grow on succinate, but not on other C4-dicarboxylates. Can J Microbiol 47:509–518. https://doi.org/10.1139/w01-041.
31. Batista S, Patriarca EJ, Tatè R, Martínez-Drets G, Gill PR. 2009. An alternative succinate (2-oxoglutarate) transport system in *Rhizobium tropici* is induced in nodules of *Phaseolus vulgaris*. J Bacteriol 191:5057–5067. https://doi.org/10.1128/JB.00252-09.
32. Zhang Y, Aono T, Poole P, Finan TM. 2012. NAD(P)+-malic enzyme mutants of *Sinorhizobium* sp. strain NGR234, but not *Azorhizobium caulinodans* ORS571, maintain symbiotic N2 fixation capabilities. Appl Environ Microbiol 78:2803–2812. https://doi.org/10.1128/AEM.06412-11.
33. diCenzo GC, Zamani M, Cowie A, Finan TM. 2015. Proline auxotrophy in *Sinorhizobium meliloti* results in a plant-specific symbiotic phenotype. Microbiology 161:2341–2351. https://doi.org/10.1099/mic.0.000182.
34. Dunn MF. 2015. Key roles of microsymbiont amino acid metabolism in rhizobia-legume interactions. Crit Rev Microbiol 41:411–451. https://doi.org/10.3109/1040841X.2013.856854.
35. Karunakaran R, Haag AF, East AK, Ramachandran VK, Prell J, James EK, Scocchi M, Ferguson GP, Poole PS. 2010. BacA is essential for bacteroid development in nodules of galegoid, but not phaseoloid, legumes. J Bacteriol 192:2920–2928. https://doi.org/10.1128/JB.00020-10.
36. Zamani M, diCenzo GC, Milunovic B, Finan TM. 2017. A putative 3-hydroxyisobutyryl-CoA hydrolase is required for efficient symbiotic nitrogen fixation in *Sinorhizobium meliloti* and *Sinorhizobium fredii* NGR234. Environ Microbiol 19:218–236. https://doi.org/10.1111/1462-2920.13570.
37. Osterås M, Finan TM, Stanley J. 1991. Site-directed mutagenesis and DNA sequence of *pckA* of *Rhizobium* NGR234, encoding phosphoenolpyruvate carboxykinase: gluconeogenesis and host-dependent symbiotic phenotype. Mol Gen Genet 230:257–269. https://doi.org/10.1007/BF00290676.
38. Kohl DH, Schubert KR, Carter MB, Hagedorn CH, Shearer G. 1988. Proline metabolism in N2-fixing root nodules: energy transfer and regulation of purine synthesis. Proc Natl Acad Sci U S A 85:2036–2040. https://doi.org/10.1073/pnas.85.7.2036.
39. Prell J, Bourdès A, Karunakaran R, Lopez-Gomez M, Poole P. 2009. Pathway of γ-aminobutyrate metabolism in *Rhizobium leguminosarum* 3841 and its role in symbiosis. J Bacteriol 191:2177–2186. https://doi.org/10.1128/JB.01714-08.
40. Yurgel SN, Kahn ML. 2005. *Sinorhizobium meliloti dctA* mutants with partial ability to transport dicarboxylic acids. J Bacteriol 187:1161–1172. https://doi.org/10.1128/JB.187.3.1161-1172.2005.
41. diCenzo GC, MacLean AM, Milunovic B, Golding GB, Finan TM. 2014. Examination of prokaryotic multipartite genome evolution through experimental genome reduction. PLoS Genet 10:e1004742. https://doi.org/10.1371/journal.pgen.1004742.
42. Finan TM, Kunkel B, De Vos GF, Signer ER. 1986. Second symbiotic megaplasmid in *Rhizobium meliloti* carrying exopolysaccharide and thiamine synthesis genes. J Bacteriol 167:66–72. https://doi.org/10.1128/jb.167.1.66-72.1986.
43. Sambrook J, Fritsch EF, Maniatis T. 1989. Molecular cloning: a laboratory manual. Cold Spring Harbor Laboratory Press, Cold Spring Harbor, NY.
44. Mitsch MJ, Cowie A, Finan TM. 2007. Malic enzyme cofactor and domain requirements for symbiotic N2 fixation by *Sinorhizobium meliloti*. J Bacteriol 189:160–168. https://doi.org/10.1128/JB.01425-06.
45. Schweizer HP. 2001. Vectors to express foreign genes and techniques to monitor gene expression in pseudomonads. Curr Opin Biotech 12:439–445. https://doi.org/10.1016/S0958-1669(00)00242-1.
46. Kovach ME, Elzer PH, Hill DS, Robertson GT, Farris MA, Roop RM, Peterson KM. 1995. Four new derivatives of the broad-host-range cloning vector pBBR1MCS, carrying different antibiotic-resistance cassettes. Gene 166:175–176. https://doi.org/10.1016/0378-1119(95)00584-1.
47. Leonard LT. 1943. A simple assembly for use in the testing of cultures of rhizobia. J Bacteriol 45:523–527.
48. Jensen HL. 1942. Nitrogen fixation in leguminous plants. I. General characters of root-nodule bacteria isolated from species of *Medicago* and *Trifolium* in Australia. Proc Linn Soc N S W 67:98–108.
49. diCenzo GC, Zamani M, Ludwig HN, Finan TM. 2017. Heterologous complementation reveals a specialized activity for BacA in the *Medicago-Sinorhizobium meliloti* symbiosis. Mol Plant Microbe Interact 30:312–324. https://doi.org/10.1094/MPMI-02-17-0030-R.
50. Vasse J, de Billy F, Camut S, Truchet G. 1990. Correlation between ultrastructural differentiation of bacteroids and nitrogen fixation in alfalfa nodules. J Bacteriol 172:4295–4306. https://doi.org/10.1128/jb.172.8.4295-4306.1990.
51. Andrews S. 2010. FastQC: a quality control tool for high-throughput sequence data. Babraham Bioinformatics, Babraham Institute, Cambridge, United Kingdom.
52. Alves-Carvalho S, Aubert G, Carrère S, Cruaud C, Brochot AL, Jacquin F, Klein A, Martin C, Boucherot K, Kreplak J, Silva C, Moreau S, Gamas P, Wincker P, Gouzy J, Burstin J. 2015. Full-length de novo assembly of RNA-seq data in pea (*Pisum sativum* L.) provides a gene expression atlas and gives insights into root nodulation in this species. Plant J 84:1–19. https://doi.org/10.1111/tpj.12967.
53. Young JPW, Crossman LC, Johnston AW, Thomson NR, Ghazoui ZF, Hull KH, Wexler M, Curson AR, Todd JD, Poole PS, Mauchline TH, East AK, Quail MA, Churcher C, Arrowsmith C, Cherevach I, Chillingworth T, Clarke K, Cronin A, Davis P, Fraser A, Hance Z, Hauser H, Jagels K, Moule S, Mungall K, Norbertczak H, Rabbinowitsch E, Sanders M, Simmonds M, Whitehead S, Parkhill J. 2006. The genome of *Rhizobium leguminosarum* has recognizable core and accessory components. Genome Biol 7:R34. https://doi.org/10.1186/gb-2006-7-4-r34.
54. Camacho C, Coulouris G, Avagyan V, Ma N, Papadopoulos J, Bealer K, Madden TL. 2009. BLAST+: architecture and applications. BMC Bioinformatics 10:421. https://doi.org/10.1186/1471-2105-10-421.
55. Langmead B, Salzberg SL. 2012. Fast gapped-read alignment with Bowtie 2. Nat Methods 9:357–359. https://doi.org/10.1038/nmeth.1923.
56. Anders S, Pyl PT, Huber W. 2015. HTSeq-a Python framework to work with high-throughput sequencing data. Bioinformatics 31:166–169. https://doi.org/10.1093/bioinformatics/btu638.
57. Love MI, Huber W, Anders S. 2014. Moderated estimation of fold change and dispersion for RNA-seq data with DESeq2. Genome Biol 15:550. https://doi.org/10.1186/s13059-014-0550-8.
58. Lohse M, Nagel A, Herter T, May P, Schroda M, Zrenner R, Tohge T, Fernie AR, Stitt M, Usadel B. 2014. Mercator: a fast and simple web server for genome scale functional annotation of plant sequence data. Plant Cell Environ 37:1250–1258. https://doi.org/10.1111/pce.12231.
59. Huerta-Cepas J, Forslund K, Szklarczyk D, Jensen LJ, Mering von C, Bork P. 29 April 2017. Fast genome-wide functional annotation through orthology assignment by eggNOG-mapper. Mol Biol Evol https://doi.org/10.1093/molbev/msx148.
60. Meade HM, Long SR, Ruvkun GB, Brown SE, Ausubel FM. 1982. Physical and genetic characterization of symbiotic and auxotrophic mutants of *Rhizobium meliloti* induced by transposon Tn*5* mutagenesis. J Bacteriol 149:114–122.
61. Johnston AWB, Beringer JE. 1975. Identification of the *Rhizobium* strains in pea root nodules using genetic markers. J Gen Microbiol 87:343–350. https://doi.org/10.1099/00221287-87-2-343.
62. diCenzo GC, Muhammed Z, Østerås M, O'Brien SAP, Finan TM. 2017. A key regulator of the glycolytic and gluconeogenic central metabolic pathways in *Sinorhizobium meliloti*. Genetics 207:961–974. https://doi.org/10.1534/genetics.117.300212.